Journal of Pharmaceutical Analysis 6 (2016) 39–48

HOSTED BY

Contents lists available at ScienceDirect

Journal of Pharmaceutical Analysis

journal homepage: www.elsevier.com/locate/jpa
www.sciencedirect.com

Original Article

The synthesis of boronic-imine structured compounds and identification of their anticancer, antimicrobial and antioxidant activities ☆

Salih Pasa [a], Safa Aydın [b], Sadık Kalaycı [b], Mehmet Boğa [c], Metin Atlan [a], Murat Bingul [c], Fikrettin Şahin [b], Hamdi Temel [a,c,*]

[a] Science and Technology Research and Application Center, Dicle University, 21280 Diyarbakir, Turkey
[b] Department of Genetics and Bioengineering, Faculty of Engineering and Architecture, Yeditepe University, Kayisdagi, 34755 İstanbul, Turkey
[c] Department of Pharmaceutical Chemistry, Faculty of Pharmacy, Dicle University, 21280 Diyarbakir, Turkey

ARTICLE INFO

Article history:
Received 7 July 2015
Received in revised form
11 November 2015
Accepted 13 November 2015
Available online 1 December 2015

Keywords:
Boronic compounds
Imine base
Anticancer activity
Antioxidant
Antimicrobial

ABSTRACT

Boronic acid compounds with different substituted groups were handled to synthesize various ligands encoded as B1, B2, B3, B4, B5, B6, B7 and B8. B5 and B7 were tested for the cytotoxic activity against the prostate cancer cells and it was found that the cell viability of cancer cells was decreased while most of the healthy cells could still be viable. 5 μM solutions of B5 and B7 decreased the cell viability to 33% and 44% whereas healthy cells were 71% and 95%, respectively, after treatment. Antimicrobial properties were explored against the bacterial and fungal microorganisms with B1, B5 and B7. The inhibition zones were evaluated for all boronic structures, and the growth inhibition zones were determined in a range of 7–13 mm diameter for different microorganism species. *Staphylococcus aureus* was the common microorganism that three boronic compounds with imine ligands showed the activity. Antioxidant features of B2, B3, B4, B5, B6, B7 and B8 were investigated by different processes such as Beta-carotene bleaching (BCB), *2,2-diphenyl picryl hydrazyl* (DPPH), *2,2'-azino-bis(3-ethylbenzothiazoline-6-sulphonic acid)* (ABTS) and CUPric reducing antioxidant capacity (CUPRAC) methods. Significant antioxidant activity was achieved by the phenyl boronic based ligands and these compounds demonstrated as much activity as standards (α-Toc and BHT). In addition, all structures were applied properly without any decomposition during the experiments. They were rather stable both in aqueous media and solid state.
© 2015 Xi'an Jiaotong University. Production and hosting by Elsevier B.V. All rights reserved. This is an open access article under the CC BY-NC-ND license (http://creativecommons.org/licenses/by-nc-nd/4.0/).

1. Introduction

Boron exists as a trace element in many kinds of vegetables, fruits, especially in nuts. Evidences show that the deficiency or excess of boron causes biological influences [1,2]. It has a significant role in hormone and enzyme reactions as well as in the mineral metabolism system for the cell membrane functions and boron is a fundamental component for the growth process of many plants. In addition to this, it has been determined as an essential necessity for human life so that it is found in human and animal tissues at mild concentrations [2]. Previous studies have shown that the deficiency of boron is responsible for the decline of plant photosynthetic capacity [3–5]. In particular, the lack of boron minerals negatively affects agricultural crops. These kinds of problems have urged researchers to focus on boron activities in living systems [6].

The inadequacy of nutritional boron has an impact on brain electrophysiology and brain behaviors. Apart from the psychological events, boronic compounds have been commonly used in cancer treatment, which is called as Boron Neutron Capture Therapy (BNCT) [7]. The treatment is briefly based on capture reaction between a neutron and ^{10}B isotope. The neutron absorption by a boronic compound supplies more energy to be efficient in the biological fraction. Boron and the neutrons cannot cause any tissue damages by themselves. Various boronic structures have been exerted in tumor and cancer therapy with limited thriving outputs. Since BNCT requires a high cost nuclear reactor, it has a restricted usage worldwide in clinical treatments [8–11].

Literature research also represents that the exchange of boron

☆ Peer review under responsibility of Xi'an Jiaotong University.

* Corresponding author at: Department of Pharmaceutical Chemistry, Faculty of Pharmacy, Dicle University, 21280 Sur/Diyarbakır, Turkey.
E-mail address: htemel@dicle.edu.tr (H. Temel).

http://dx.doi.org/10.1016/j.jpha.2015.11.003
2095-1779/© 2015 Xi'an Jiaotong University. Production and hosting by Elsevier B.V. All rights reserved. This is an open access article under the CC BY-NC-ND license (http://creativecommons.org/licenses/by-nc-nd/4.0/).

atom has an important effect on antioxidant enzymes. Most of the plant studies have shown that excess of boron stimulates the antioxidant enzymes and particularly activates the enzymes related to ascorbate cycle [12–15].

2. Materials and methods

2.1. Materials and instrumentation

In the present research, eight new boronic compounds containing imine (C=N) ligands (B1–B8) were synthesized by the reaction of aromatic amines with phenyl boronic acids bearing aldehyde group [16,17]. The structural identification of synthesized compounds was done by various spectroscopic methods such as nuclear magnetic resonance (^{1}H and ^{13}C NMR), liquid chromatography–mass spectroscopy (LC–MS), Fourier transform infrared (FTIR) spectroscopy, ultraviolet visible (UV–vis) spectroscopy, elemental analysis and scanning electron microscope (SEM). Then, these boronic compounds were explored for the anticancer, antimicrobial and antioxidant purposes. Prostate cancer cells were treated with boronic compounds and the cytotoxic behaviors were identified. The toxicity levels of these compounds against the healthy cells were also explored in the present work. Antimicrobial studies were carried out on different kinds of microorganisms such as *Staphylococcus aureus, Escherichia coli,* Methicillin-resistant *Staphylococcus aureus* (*MRSA*), *Pseudomonas aeruginosa, Candida albicans, and Aspergillus niger*. The boronic-imine structured compounds have shown considerable efficiencies on microorganisms in the previous researches in last decade [16–20]. The antioxidant behavior was investigated by using a variety of methods such as β-carotene bleaching (BCB), *2,2-diphenyl-1-picrylhydrazyl* (DPPH), CUPric reducing antioxidant capacity (CUPRAC) and *2,2′-azino-bis(3-ethylbenzothiazoline-6-sulphonic acid*) (ABTS).

All the reagents and chemicals were supplied by Sigma-Aldrich (Steinheim, Germany) and Fluka (St. Gallen, Switzerland). All the synthetic pathways were conducted under Ar atmosphere in appropriate glasswares unless otherwise stated. ^{1}H and ^{13}C NMR spectra were recorded on a Bruker AV400 spectrometer (Karlsruhe, Germany) with δ referenced to external tetramethylsilane (TMS). FTIR spectra were recorded on an attenuated total reflectance (ATR) apparatus on a Perkin Elmer Spectrum 100 Fourier transform spectrophotometer. LC–MS analyses were performed by a Shimadzu LC/MS 8040 instrument (Kyoto, Japan). Elemental analysis of carbon, hydrogen and nitrogen was carried out on a Costech Combustion System CHNS-O instrument (Cernusco S/Nav.-MI-Italy). Melting points were measured by a Barnstead Electrothermal 9100 (San Francisco, USA). SEM images were taken by a FEI Quanta 250 FEG instrument (Eindhoven, Netherlands).

2.2. Methods

2.2.1. Synthesis of boronic derivative compounds

2.2.1.1. Synthesis of B1 (2-(6-methoxynaphthalen-2yl)benzo[d][1,3,2] dioxaborol4-ol). Pyrogallol (0.126 g, 1 mmol) dissolved in 20 mL of tetrahydrofurane (THF) was added into the solution of 6-methoxynaphthalene (0.202 g, 1 mmol) prepared in ethanol (20 mL) and heated under reflux for 48 h. The brownish precipitate was obtained after removal of the solvent, which was washed with ethanol and dried in an oven. The product is soluble in acetone: dimethyl sulfoxide (DMSO) (1:1, v/v). *M*p (Melting point): 198–202 °C. ^{1}H NMR (ppm, DMSO-d_6): δ 5.44 (Ph–OH), 3.95 (Naph–OCH_3). FTIR-ATR (cm^{-1}): 1383–1324 ν(B–O), 723 ν(B–Ph). *m/z*: 291.08 [M−H$^+$] $C_{17}H_{13}BO_4$ (M_W:292.0922 g/mol). UV–vis (nm): λ_1=296 (ε=2.96 × 10^3), λ_2=311 (ε=3.11 × 10^3), in acetone: DMSO (1:1). Elemental analysis (%): Found (Calc.) C 70.86 (69.90), H 4.29 (4.49) (Scheme 1).

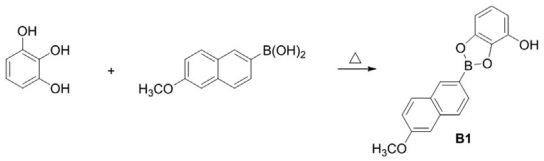

Scheme 1. Synthesis of B1.

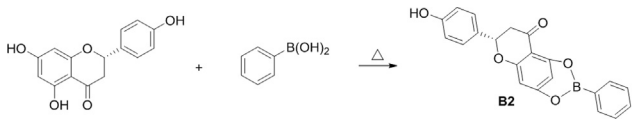

Scheme 2. Synthesis of B2.

2.2.1.2. Synthesis of B2 (Naringenin based boronic acid). Naringenin (0.275 g, 1 mmol) in 30 mL of absolute ethanol and phenyl boronic acid (0.121 g, 1 mmol) in 20 mL of ethanol were mixed in a one-necked flask and heated under reflux at 100 °C for 24 h. The yellow solid product was obtained after removal of the solvent and water, which was washed with ethanol and water, and then dried in an oven. The product is soluble in ethanol and DMSO. Mp: 210 °C. ^{1}H NMR (ppm, DMSO-d_6): δ 5.44 (Ph–OH), 6.52–8.01 (Ph–H). FTIR-ATR (cm^{-1}):1364–1334 ν(B–O), 759 ν(B–Ph). *m/z*: 359 [M+H$^+$] $C_{21}H_{15}BO_5$ (M_W: 358.15 g/mol). UV–vis (nm): λ_1=216 (ε =2.16 × 10^3), λ_2=334 (ε=3.34 × 10^3), in ethanol. Elemental analysis (%): Found (Calc.) C 67.13 (67.42), H 4.08 (4.02) (Scheme 2).

2.2.1.3. Synthesis of B3 (3-((4-(hydrazine carbonyl) phenyl imino) methyl) phenyl boronic acid). 4-amino benzoic hydrazide (0.151 g, 1 mmol) in 20 mL of absolute ethanol and 3-formyl phenyl boronic acid (0.149 g, 1 mmol) in 15 mL of ethanol were mixed in a one-necked flask and heated under reflux at 100 °C for 24 h. The yellow solid product was precipitated after removal of the solvent and water, which was washed with ethanol and water, and then dried in an oven. The product is soluble in ethanol and DMSO. *M*p:350–355 °C. ^{1}H NMR (ppm, DMSO-d_6): δ 8.39 (CH=N), 5.77 (Ph–$B(OH)_2$). FTIR-ATR (cm^{-1}): 3300–3200 (BO–H), 759 ν(B–Ph), 1601 ν(CH=N). *m/z*: 284 [M+H$^+$] $C_{14}H_{14}N_3O_3B$ (M_W: 283.09 g/mol). UV–vis(nm): λ_1=202 (ε=2.02 × 10^3), λ_2=321 (ε=3.21 × 10^3), in ethanol. Elemental analysis (%): Found (Calc.) C 60.16 (59.40), H 3.17 (3.68), N 14.0 (14.34) (Scheme 3).

2.2.1.4. Synthesis of B4 (3-((2,6-dimethoxy phenyl imino) methyl) phenyl boronic acid). 2,6-dimethoxy aniline (0.153 g, 1 mmol) in 20 mL of absolute ethanol and 3-formyl phenyl boronic acid (0.149 g, 1 mmol) in 15 mL of ethanol were mixed in a one-necked flask and heated under reflux at 100 °C for 24 h. The yellow solid product was isolated after removal of the solvent and water, which was washed with ethanol and water, and then dried in an oven. The product is soluble in ethanol and DMSO. *M*p: 230–240 °C. ^{1}H NMR (ppm, DMSO-d_6): δ 8.61 (CH=N), 5.05 (Ph–$B(OH)_2$). FTIR-ATR(cm^{-1}): 3371 (BO–H), 1585 ν(CH=N). *m/z*: 286 [M−H$^+$] $C_{15}H_{16}NO_4B$ (M_W: 287.12 g/mol). UV–vis(nm): λ_1=251 (ε =2.51 × 10^3), λ_2=330 (ε=3.30 × 10^3), in ethanol. Elemental analysis (%): Found (Calc.) C 63.92 (63.19), H 5.25 (5.66), N 4.87 (4.91) (Scheme 4).

2.2.1.5. Synthesis of B5 (3-((4-acetyl phenyl imino)methyl) phenyl boronic acid). 4-amino acetophenone (0.135 g, 1 mmol) in 15 mL of absolute ethanol and 3-formyl phenyl boronic acid (0.149 g, 1 mmol) in 15 mL of ethanol were mixed in a one-necked flask and

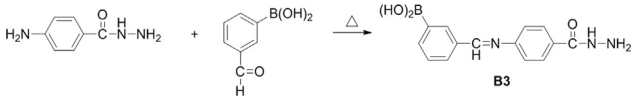

Scheme 3. Synthesis of B3.

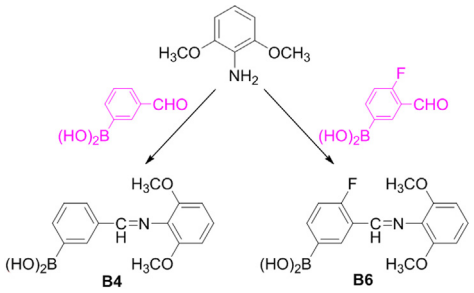

Scheme 4. Synthesis of B4 and B6.

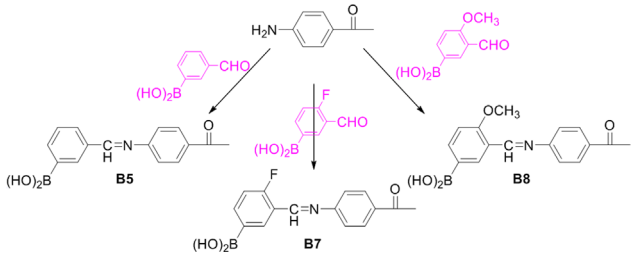

Scheme 5. Synthesis of B5, B7 and B8.

heated under reflux at 100 °C for 24 h. The reddish solid product was isolated after removal of the solvent and water, which was washed with ethanol and water, and then dried in an oven. The product is soluble in ethanol and DMSO. *M*p: 110–120 °C. ^{1}H NMR (ppm, DMSO-d_6):δ 8.63 (CH=N), 4.38 (Ph–B(OH)$_2$). FTIR-ATR (cm^{-1}):3344 (BO–H), 698 ν(B–Ph), 1623 ν(CH=N). *m*/*z*:268 [M+H$^+$] $C_{15}H_{14}NO_3B$ (M_W:267.09 g/mol). UV–vis(nm):λ_1=202 (ε =2.02 × 10^3), λ_2=398 (ε=3.98 × 10^3), in ethanol (Scheme 5).

2.2.1.6. Synthesis of B6 (3-((2,6-dimethoxy phenyl imino)methyl)-4-fluoro phenyl boronic acid). 4-flouro-3-formyl phenyl boronic acid (0.167 g, 1 mmol) in 20 mL of absolute ethanol and 2,6-dimethoxy aniline (0.153 g, 1 mmol) in 15 mL of ethanol were mixed in a one-necked flask and heated under reflux at 100 °C for 24 h. The dark brown solid product was obtained after removal of the solvent and water, which was washed with ethanol and water, and then dried in an oven. The product is soluble in ethanol and DMSO. *M*p: > 250 °C. ^{1}H NMR (ppm, DMSO-d_6): δ=8.70 (CH=N), δ=4.57 (Ph–B(OH)$_2$). FTIR-ATR (cm^{-1}): 3374 (BO–H), 1583 ν(CH=N), 1336 (Ph–F). *m*/*z*:304 [M+H$^+$] $C_{15}H_{15}NO_4BF$ (M_W:303.09 g/mol). UV–vis (nm): λ_1=212 (ε=2.12 × 10^3), λ_2=340 (ε=3.40 × 10^3), in ethanol. Elemental analysis (%): Found (Calc.) C 61.67 (61.44), H 3.90 (4.09), N 5.16 (4.97) (Scheme 4).

2.2.1.7. Synthesis of B7 (3-((4-acetylphenyl imino) methyl)-4-fluoro phenyl boronic acid). 4-amino acetophenone (0.135 g, 1 mmol) in 15 mL of absolute ethanol and 4-flouro-3-formyl phenyl boronic acid (0.167 g, 1 mmol) in 15 mL of ethanol were mixed into a one-necked flask and heated under reflux at 100 °C for 24 h. The reddish solid product was collected after removal of the solvent and water, which was washed with ethanol and water, and then dried in an oven. The product is soluble in ethanol and DMSO. *M*p: 116–120 °C. ^{1}H NMR (ppm, DMSO-d_6): δ 8.77 (CH=N), 4.38 (Ph–B(OH)$_2$). FTIR-ATR (cm^{-1}): 3348 (BO–H), 1623 ν(CH=N), 1336 (Ph–F). *m*/*z*: 286 [M+H$^+$] $C_{15}H_{13}NO_3BF$ (M_W: 285.08 g/mol). UV–vis(nm): λ_1=203 (ε=2.03 × 10^3), λ_2=323 (ε=3.23 × 10^3), in ethanol (Scheme 5).

2.2.1.8. Synthesis of B8 (3-((4-acetyl phenyl imino)methyl)-4-methoxy phenyl boronic acid). 4-amino acetophenone (0.135 g, 1 mmol) in 15 mL of absolute ethanol and 4-methoxy-3-formyl phenyl boronic acid (0.179 g, 1 mmol) in 20 mL of ethanol were mixed into a one-necked flask and heated under reflux at 100 °C for 24 h. The yellow solid product was obtained after removal of the solvent and water, which was washed with ethanol and water, and then dried in an oven. The product is soluble in ethanol and DMSO. *M*p: 155 °C. ^{1}H NMR (ppm, DMSO-d_6): δ 8.84 (CH=N), 4.38 (Ph–B(OH)$_2$). ^{13}C NMR (ppm, DMSO-d_6): 163.48 (CH=N), 123.31 (Ph–C–B(OH)$_2$). FTIR-ATR (cm^{-1}): 3306 (BO–H), 1620 ν(CH=N). *m*/*z*: 298 [M+H$^+$] $C_{16}H_{16}NO_4B$ (M_W: 297.11 g/mol). UV–vis (nm): λ_1=204 (ε=2.04 × 10^3), λ_3=325 (ε=3.25 × 10^3), in ethanol. Elemental analysis (%): Found (Calc.) C 61.29 (61.68), H 4.91 (4.43), N 4.24 (4.51) (Scheme 5).

2.2.2. Anticancer assay

The anticancer activity of boronic compounds containing imine ligands was evaluated by using PC-3 (Human Prostate Cancer Cells-ATCC® CRL-1435™) and L929 cells (Mouse Fibroblast Cells-ATCC® CCL-1™) as healthy cell line. Four concentrations (0.5, 1, 2, and 5 μM) of boronic compounds were prepared in Dulbecco's modified Eagle's medium (DMEM, Invitrogen, USA) containing 10% fetal bovine serum (Invitrogen, USA), and 1% of penicillin, streptomycin, and amphotericin (Lonza, USA). PC-3 and L929 cells were seeded onto 96-well plates at a concentration of 5000 cells/well, and then incubated at 37 °C in a humidified air atmosphere with 5% CO_2 for 24 h for cell attachment. The prepared compounds were added into the cultured cells, and incubated for 24, 48 and 72 h, respectively. Cell viability was measured by the 3-(4,5-dimethyl-thiazol-2-yl)-5-(3-carboxy-methoxy-phenyl)-2-(4-sulfo-phenyl)-2H-tetrazolium (MTS)-assay (CellTiter96 AqueousOne Solution; Promega, Southampton, UK) according to the manufacturer's instructions. Cells were incubated with the MTS solution for 2 h at 37 °C and absorbance was measured at 490 nm using an ELISA plate reader (Biotek, Winooski, VT).

2.2.3. Disc-diffusion assay

Antimicrobial properties of boronic compounds containing imine ligands were investigated against *E. coli* ATCC 25922, *Pseudomonas aeruginosa* ATCC 27853, *Staphylococcus aureus* ATCC 25923, Methicillin-resistant *Staphylococcus aureus*, *C. albicans* and *A. niger* by using disc-diffusion assay as described in the literature [21]. For this aim, 100 μL of freshly prepared microbial suspensions containing 10^8 CFU/mL of bacteria, 10^6 CFU/mL of yeast and 10^4 spore/mL of fungi were spread on nutrient agar, sabouraud dextrose agar and potato dextrose agar, respectively. Black discs (6 mm) impregnated with boron derivatives (20 μL) of the specified concentrations were placed on the inoculated plates. Distilled water (20 μL) was used as negative control. Oflaxacin (5 μg/disc) and nystatin (100 μg/disc) were used as positive controls for bacterial and fungal species tested, respectively. The inoculated plates were incubated at 36 ± 1 °C for 24 h for bacterial strains and 48 h for yeast, and 27 ± 1 °C for 72 h for fungal isolate. Antimicrobial activity was determined by measuring zone of inhibition around the discs.

2.2.4. Antioxidant implementation

The antioxidant activity of boronic based compounds were investigated by four common methods, BCB, DPPH, ABTS

and CUPRAC [13,14,22–26].

BCB process is based on the linoleic acid test system derived from the oxidation of linoleic acids by measuring the inhibitions of conjugated diene hydroperoxides. 10 mg of each compound was dissolved in 10 mL of absolute ethanol to prepare the stock solutions. 2, 5, 10 and 20 μL of stock solutions were diluted into 40 μL with the absolute ethanol. Then 160 μL of β-carotene solutions were added into each well in the micro plate. As soon as they were mixed, the absorbance was measured at 490 nm at the beginning. Then they were kept at 50 °C for 120 min. The ranges of BCB were calculated according to the Eq. (1):

$$R = \ln(a/b)/t \quad (1)$$

where ln is the natural logarithm; a is the initial absorbance; b is the incubation; t is the time (min).

The total antioxidant activities were also calculated as percentages according to the control compound using Eq. (2):

$$\text{Total antioxidant activity (\%Inhibition)} = \left[\left(R_{\text{control}} - R_{\text{sample}}\right)/R_{\text{control}} \right] \times 100 \quad (2)$$

where R_{control} is the color bleaching range of control, and R_{sample} is the color bleaching range of sample.

Each of the boronic samples was applied three times. Alpha-tocopherol (α-Toc) and di-butyl-hydroxy toluene (BHT) were used as standard compounds.

DPPH is commonly used as control material for the evaluation of molecules which can act as radical scavengers in the antioxidant activity experiments. 10 mg of each compound was dissolved in 10 mL of absolute ethanol to prepare the stock solutions. 2, 5, 10 and 20 μL of stock solutions were diluted into 40 μL with the absolute ethanol. Then 160 μL of DPPH solutions were added into each well in the micro plate. After incubation under dark condition at room temperature, the absorbances were measured at 517 nm. Free radical scavenging activities (% Inhibition) were calculated according to Eq. (3):

$$\%\text{Inhibition} = (A_{\text{control}} - A_{\text{sample}})/A_{\text{control}} \times 100 \quad (3)$$

where A is the absorbance.

Each of the samples was applied three times to verify the results. α-Toc and BHT were also used as standard compounds.

ABTS is an assay depending on the radical cation decolorization. In this assay, the addition of antioxidants into the solution including radical cation form of the ABTS converted this compound back into the neutral form in a variety of time-sclae. The different antioxidant efficiencies of boronic compounds were responsible for this issue. The degree of decolorization as percentage inhibition of $ABTS^{\cdot+}$ radical cation is obtained as a function of time and concentration, and calculated relative to the activity of α-Toc and BHT. The preparation of stock solutions was carried out by dissolving 10 mg of each compound in 10 mL of absolute ethanol. 2, 5, 10 and 20 μL of stock solutions were diluted into 40 μL with the absolute ethanol. Then 160 μL of ABTS solutions were added into each well in the micro plate. After keeping them in tightened place for 6 min in the absence of sunlight at room temperature, the absorbances were measured at 734 nm. ABTS radical cation decolorization activities as % Inhibition were determined by using the Eq. (4):

$$\%\text{Inhibition} = (A_{\text{control}} - A_{\text{sample}})/A_{\text{control}} \times 100 \quad (4)$$

where A is the absorbance.

CUPRAC method comprises the reduction of Cu(II)-Neocuproine into its colored form Cu(I)-Neocuproine chelate in the presence of antioxidant compounds. The absorbance at 450 nm was measured when the complex was obtained. Cu(II), Neocuproine and NH_4OAc were added into the prepared solutions to adjust the concentrations as 10, 25, 50, and 100 μg/mL. The absorbance values were compared with the standard molecules α-Toc and BHT. Each of samples was applied three times to verify the results.

3. Results and discussion

3.1. Structure identification of B1-8 compounds

In the ^{1}H NMR spectrum of B1, a singlet resonances at 5.44 ppm and 3.95 ppm corresponds to hydroxyl proton on aromatic ring and methoxy group on naphthalene boronic acid structure [27–29]. The exact mass was found as m/z 291.0838 corresponds to the B1 structure with $[M-H^+]$ at negative scan by liquid chromatography mass spectrometry with ion trap time of flight (LC–MS–IT–TOF) (Fig. 1).

Stretching vibrations at a range of 1383–1324 cm^{-1} and 723 cm^{-1} substantiated the boron binding (B–O) over oxygen atoms and the B–Ph bond [28,30,31]. Electronic transitions such as $\pi \rightarrow \pi^*$ and $n \rightarrow \pi^*$, are based on the aromatic ring and the oxygen atoms which can be understood from the absorption peaks at 296 and 311 nm. SEM and TGA results revealed important data about the physical properties of B1. The surface morphology seemed like cotton or tobacco pieces with heterogeneous dispersion. B1 was analyzed under low vacuum (100 Pa) mode with 1500 times magnification [32–35]. Its thermogram explains the stable nature of the compound up to 282 °C. The weight loss was determined in two steps as 58% and 23.5% at different temperatures (Fig. 2).

The ^{1}H NMR spectrum of B2 represented a singlet resonance at 5.44 ppm belonging to Ph–OH and the aromatic protons appear between 6.52 and 8.01 ppm [27–29,36]. The exact mass value was proved by mass spectrum that shows the most abundance approximately 10^6 intensity at 359 with the positive scan $[M+H^+]$. Similarly, stretching vibrations were assigned at the expected regions for boron binding (B–O) and the B–Ph vibration. $\pi \rightarrow \pi^*$ and $n \rightarrow \pi^*$ transitions were obtained at 216 and 334 nm, respectively [37–39]. The physical appearance of compound in SEM looked like crumbled rocks with a single phase. Thermal stability and weight loss experiment of B2 were also evaluated by TGA [33–35] and it was found that it was quite stable up to 400 °C. Two step decompositions were depicted on the thermogram. (Fig. 2).

Structure of B3 was confirmed by resonances at 8.39 ppm for azomethine proton (–CH=N–), 5.77 ppm for boronic protons, 4.36 ppm for secondary amine proton (N–H), 1.06 ppm for the primary amine protons (NH_2) with the ^{1}H NMR spectrum [32,33,41,45]. m/z:284 $[M+H^+]$ showed the molecular weight of B3 in LC–MS analysis. The stretching vibration appeared at 3300–3200 cm^{-1} due to the acidic proton, primary amine at 3342–3218 cm^{-1}, –CH=N stretching vibration at 1601 cm^{-1} in the FTIR spectrum. Electronic transitions of B3 were determined at 202 and 321 nm due to the $\pi \rightarrow \pi^*$ and $n \rightarrow \pi^*$ transition, respectively [33,36,37,39]. Surface structure seemed like severed rock fragments in the SEM image. The thermal behavior of boronic based structure was also meaningful due to the boron nature [33,35,41]. There was no weight loss up to 310 °C and 62.85% of weight loss was calculated after it was heated to 800 °C under nitrogen atmosphere (Fig. 2).

The ^{1}H NMR spectrum of B4 displayed a singlet resonance at 8.61 ppm for imine proton (–CH=N–) and 5.05 ppm for Ph–$B(OH)_2$ protons [23,31,35]. Molecular weight was found as m/z:286 by negative scan mode $[M-H^+]$ with $C_{15}H_{16}NO_4B$ formula. The peak intensity corresponding to B4 was approximately 7.5×10^6 in LC–MS. The free boronic (BO–H) stretching vibration at 3371 cm^{-1}, B–Ph stretching at 704 cm^{-1} and azomethine

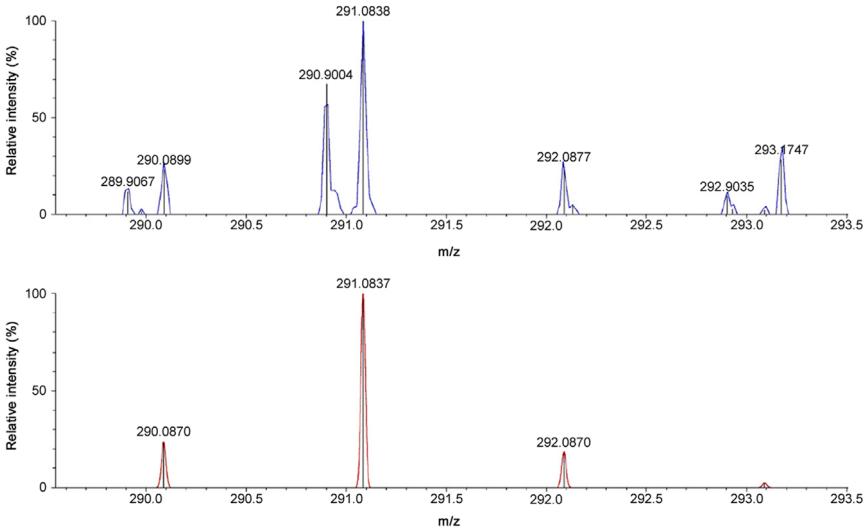

Fig. 1. LC–MS–IT–TOF spectra of B1.

stretching (–CH=N) at 1585 cm^{-1} supported the proposed structure [28,37,42]. Two broad bands can be seen in the UV region at 251 nm and 330 nm which may be attributed to the $\pi \rightarrow \pi^*$ and $n \rightarrow \pi^*$ electronic transitions, respectively [38,39]. SEM and TGA results showed data about the physical features of B4. The SEM image of B4 described the different particle sizes and agglomerated forms as a result of the amorphous nature of B4. TGA analysis clarified the thermal stability of boronic based ligands, which was quite stable up to 346 °C due to the insignificant weight loss [33–35,43]. After heated at 800 °C, the decomposition was calculated in two steps with the ranges of 37%–18% (Fig. 2).

The ^1H NMR spectrum of B5 illustrated the resonances at 8.63 ppm and 4.38 ppm corresponding to imine proton (–CH=N–) and boronic protons (Ph–B–$(OH)_2$), respectively [28,40]. The molecular weight was determined as *m/z*:268 by positive scan mode $[M+H^+]$. Stretching vibrations at 3344 cm^{-1}, 698 cm^{-1} and 1623 cm^{-1} may be assigned to BO–H, B–Ph, CH=N bonds, respectively and the peak at 759 cm^{-1} was assigned to the B–Ph vibration [28,30,31,36,44]. $\pi \rightarrow \pi^*$ and $n \rightarrow \pi^*$ transitions were obtained at 202 nm and 398 nm, respectively. The physical semblance of compound in SEM showed crumbled rocks with homogenous dispersion [32–35]. Thermal stability was found quite fine up to 300 °C and the thermogram of B5 illustrated the single step decomposition (Fig. 2).

The analogue B6 was also characterized by ^1H NMR spectrum with meaningful resonances at 8.70 ppm and 4.57 ppm corresponding to imine proton (–CH=N) and boronic protons (Ph–$B(OH)_2$), respectively [27,28,40]. *m/z*:304 $[M+H^+]$ proved the mass value of B6 with $C_{15}H_{15}NO_4BF$ formula by applying positive scan analysis in LC–MS. The stretching vibration of free boronic group appeared at 3374 cm^{-1}. The peaks at 1583 cm^{-1} and 758 cm^{-1} also showed –CH=N and B–Ph stretchings, respectively. Electronic transitions of B6 were at 212 and 340 nm as $\pi \rightarrow \pi^*$ and $n \rightarrow \pi^*$ transition, respectively [28,31,37,39]. Surface morphology seemed like shredded leaf pieces in SEM image. It was investigated under 109 Pa pressure with 6000 times magnification [32,33,43,45]. The thermal behavior of boronic based compound was found stable up to 230 °C. Then it started to decompose in two steps with the ranges from 31% to 35% (Fig. 2)

The structures of B7 and B8 are different from each other due to the existence of different substituents on the structure, namely, fluoride and methoxy groups. Resonances at 8.84 ppm and 8.77 ppm corresponded to azomethine protons (–CH=N–) and the peak at 4.38 ppm indicated the boronic acid protons [28,29,40,46]. Electronic behaviors obtained by UV–vis presented two electronic transitions arose from $\pi \rightarrow \pi^*$ to $n \rightarrow \pi^*$ at 203–323 nm and 204–325 nm, respectively [37]. Mass spectra of B7 and B8 showed similar results with the values of *m/z*:286 $[M+H^+]$ $C_{15}H_{13}NO_3BF$ and *m/z*:298 $[M+H^+]$ $C_{16}H_{16}NO_4B$, respectively. They demonstrated high intensities (1×10^5 and 1.8×10^7) by applying SIM (Selected Ion Monitoring) scan experiment in LC–MS. The stretching vibrations for the BO–H, B–Ph and CH=N bonds were defined at 3306–3348 cm^{-1}, 729–745 cm^{-1} and 1620–1623 cm^{-1}, respectively [28,36]. The SEM image of B7 seemed like crumbled rocks with heterogeneous distribution while B8 looked like grinded crystal pieces with single phase and homogeneous spread. Both particle sizes were determined approximately 10 μm with the 6000 times enlargement. Thermal can be understood up to 220 °C and 143 °C by TGA thermograms [33–35,43]. Decompositions of B7 and B8 are depicted in Fig. 2.

3.2. Anticancer activity

According to the results from the screening, the prostate cancer cells (PC-3) were found to be the more sensitive cells towards the treatment of B5 and B7 compounds, while these compounds showed no toxicity on the healthy L929 cells (Fig. 3). The treatment of compound B5 suggested a time- and dose-dependent pattern and this compound displayed the highest toxicity on the cell viability of PC-3 at 5 μM with the values of 33% on the 72 h time period. However, it had no effect on the viability of L929 cells and at the same time period and concentration of compound B5, 71% viable cells were observed (Fig. 3).

Interestingly, the identical time- and dose-dependent pattern was observed in the case of compound B7 against both cancer cell and healthy cell lines. The compound B7 showed similar cell viability differentials with the values of 44% for the prostate cancer cells (PC-3) at the concentrations of 5 μM and at 72 h. This compound could reduce the viability of healthy L929 cells by the value of 5% (95% viable cells) at 72 h (Fig. 4).

The results showed that boronic compounds containing imine ligands specifically exhibited toxicity on prostate cancer cells. Comparison of the cytotoxic activity of these two compounds against cancer cells and toxicity levels against the healthy cells revealed that the cancer cells were more sensitive to the boronic compounds with the imine functionality compared to the normal cells. Consequently, these two compounds could be entitled as promising anticancer drug candidates for the drug design in cancer research.

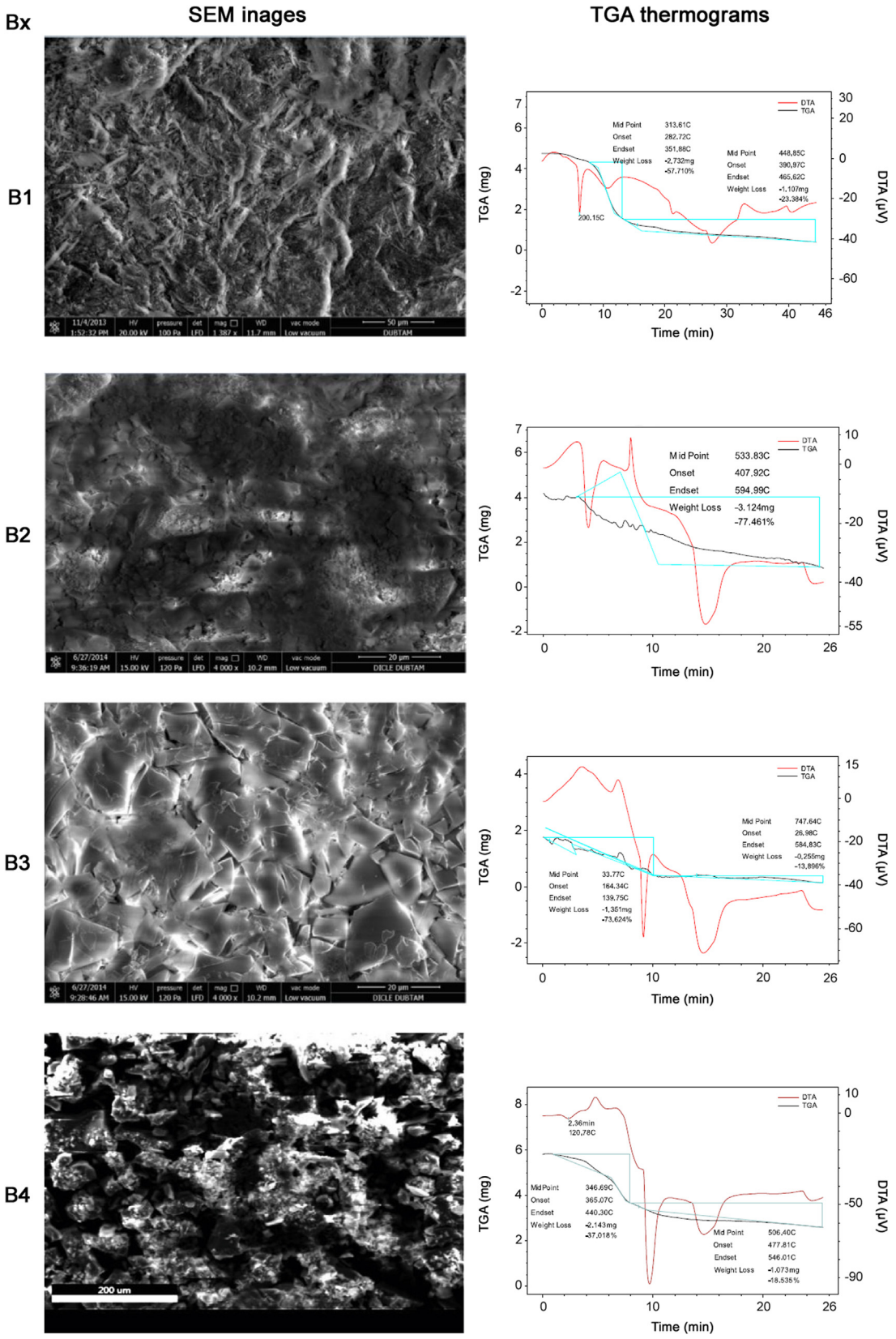

Fig. 2. SEM images and TGA thermograms of compounds.

3.3. *Antimicrobial activity*

The results revealed that boronic compounds displayed different antimicrobial activities on bacteria, yeast and fungi tested (Table 1). B1 coded boron containing imine ligand displayed moderate effect with a wide-range antimicrobial activity. It was found to be effective against both methicillin-sensitive and methicillin-resistant *S. aureus*, *C. albicans* and *A. niger*. The similar growth inhibitions were

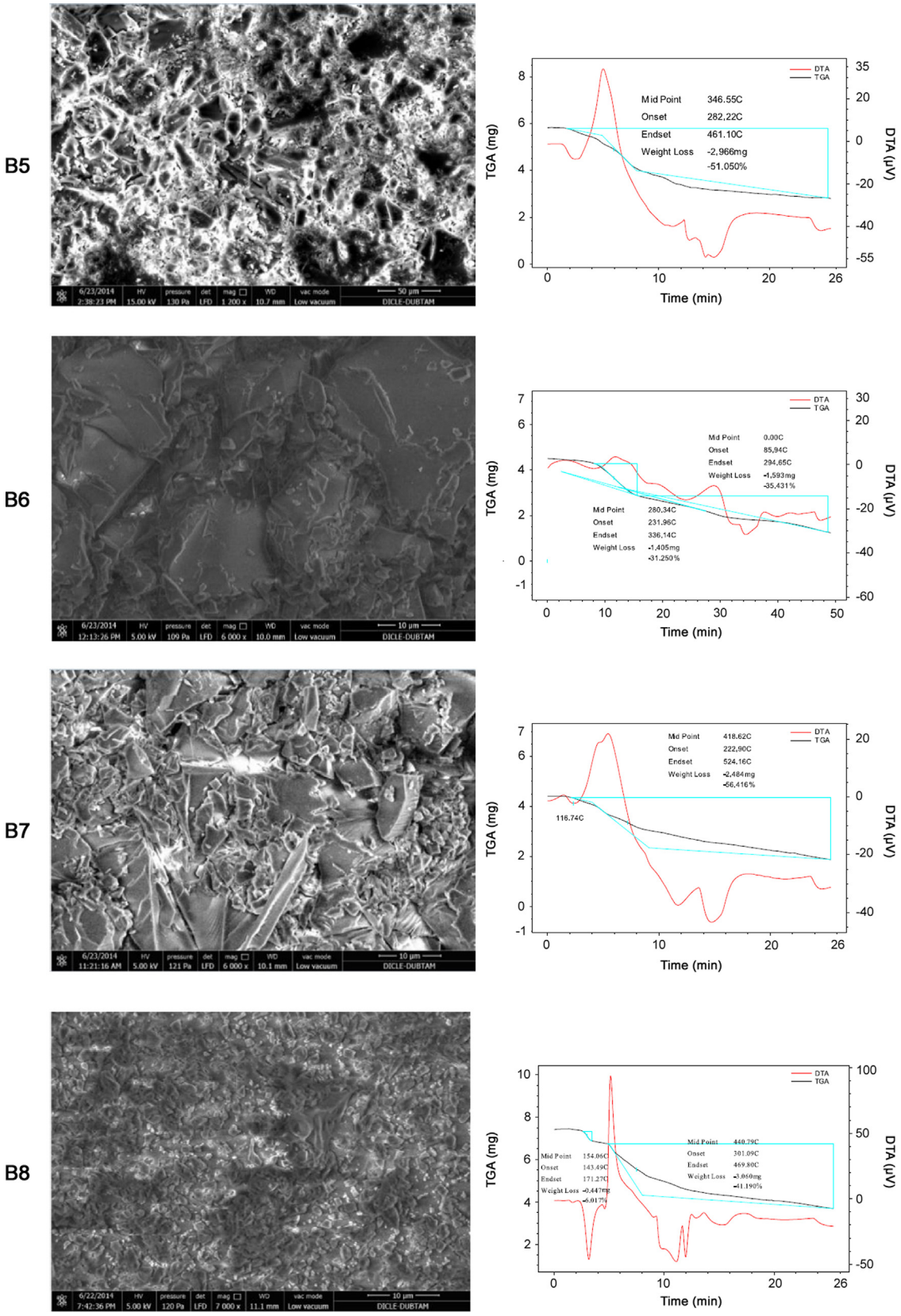

Fig. 2. (*continued*)

measured in the case of methicillin-sensitive *S. aureus* and methicillin-resistant *S. aureus* with the inhibition zone diameters of 7.5 mm and 7.0 mm, respectively whereas the growth inhibition zone was measured as 8.0 mm and 10.0 mm in case of the *C. albicans* and *A. niger*. On the other hand, B5 displayed antibacterial activity against *S. aureus* and methicillin-resistant *S. aureus* with the values of 13 mm and 9 mm, respectively. This compound could not inhibit the rest of the microorganisms. B7 coded boronic compound with imine ligand

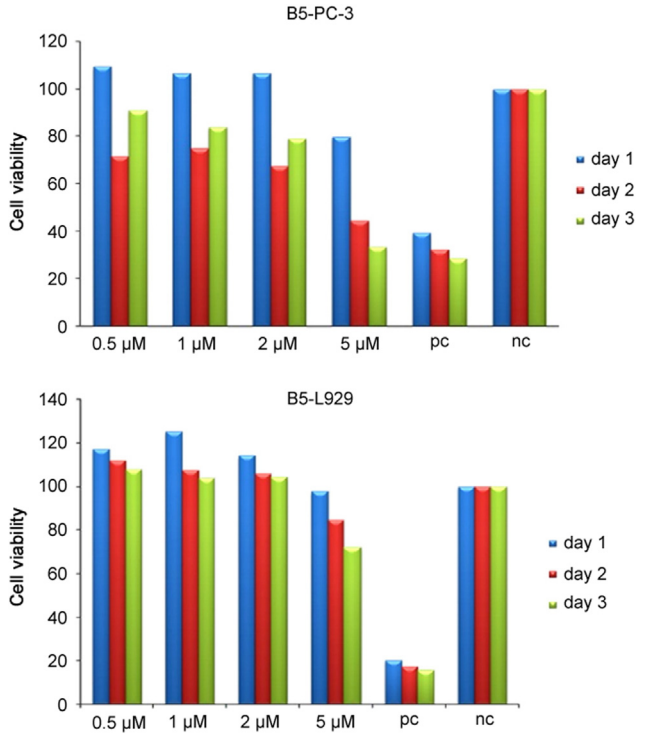

Fig. 3. Cell viability of PC-3 and L929 treated with B5 (PC-3: human prostate cancer cells, L929: mouse fibroblast cells as healthy cell line, nc: negative control, pc: positive control).

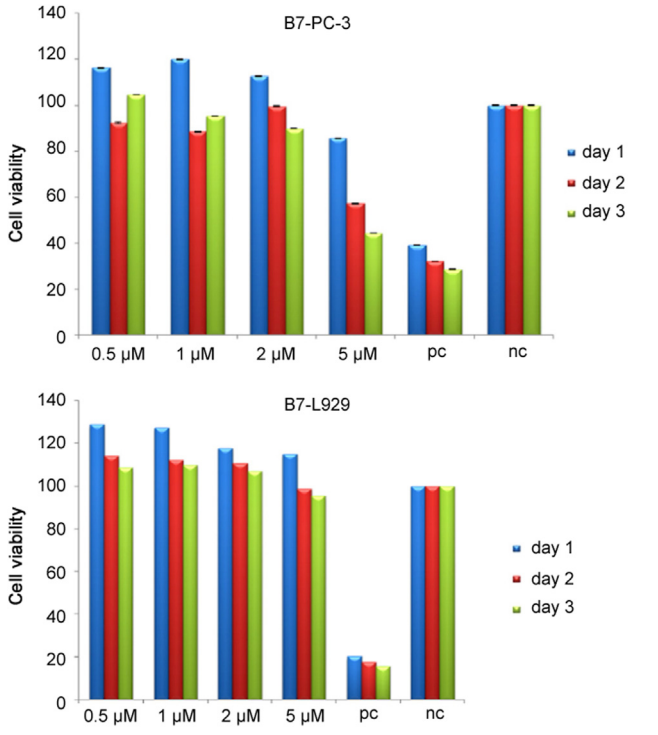

Fig. 4. Cell viability of PC-3 and L929 treated with B7 (PC-3: human prostate cancer cells, L929: mouse fibroblast cells as healthy cell line, nc: negative control, pc: positive control).

had the weakest antimicrobial activity as it only inhibited *S. aureus* growth with a zone diameter of 8.5 mm (Table 1).

3.4. Antioxidant activity

According to the results from the BCB method, B3, B4 and B6 were identified as the most effective compounds while B5 showed a moderate activity and B7 was found to be the least active compound for this assay. It can be seen from Fig. 5 that B3, B4 and B6 demonstrated better activity than the standard α-Toc whereas the comparison between the standard BHT and these three compounds showed that at 100 μg/mL concentrations there was less than 15% difference for each compound. The antioxidant activity pattern was found identical in the case of compounds B3 and B4 as the higher concentrations showed the better activity. On the other hand B6 was identified as the best compound due to the more than 80% activity at 25 μg/mL (Fig. 5).

The second antioxidant assay by using the DPPH showed no significant efficiencies in case of the all boronic compounds with imine ligands. It was considered that B2 and B3 were the least active compounds with the 10% antioxidant activity at 100 μg/mL concentrations. B4 and B6 showed similar antioxidant activity pattern as the higher concentrations showed better activity. However, the maximum amount of antioxidant activity was achieved around 25% in the case of compound B4 at 100 μg/mL and almost 40% in the case of compound B6 (Fig. 6).

ABTS radical cation quenching assay displayed distinguished results for B2, B4 and B6. These compounds represented identical antioxidant activity pattern with the both standards α-Toc and BHT at the concentrations of 25, 50 and 100 μg/mL (Fig. 7). Furthermore the antioxidant activities of these three compounds at 10 μg/mL concentrations were identified higher than both of the standards. However, in the case of compounds B3 and B5, the antioxidant activities were determined as moderate, the compounds B7 and B8 showed no activity for this assay.

Table 1
Antimicrobial activities of boronic compounds on different microorganisms by disc-diffusion assay* (SD ± 0.5–1.0 mm).

Microorganisms	Inhibition zone diameter (mm)			Positive control
	B1	B5	B7	
Staphylococcus aureus ATCC25923	7.5 ± 0.5	13 ± 1	8.5 ± 0.5	26 ± 1
Escherichia coli ATCC25922	–	–	–	28 ± 3
Methicillin-resistant *Staphylococcus aureus (MRSA)*	7 ± 0	9 ± 1	–	18 ± 1
Pseudomonas aeruginosa ATCC27853	–	–	–	22 ± 2
Candida albicans	8 ± 0	–	–	19 ± 2
Aspergillus niger	10 ± 0	–	–	24 ± 1

* Concentration of boronic compounds is 5 mg/mL, positive control: Oflaxacin (5 μg/disc) and nystatin (100 μg /disc) for bacterial and fungal species, respectively.

CUPRAC process was also applied to identify the antioxidant activity of boron complexes. B6 coded compound was reported as the most efficient compound among the tested compounds. The comparison of this compound with the standard substances BHT and α-Toc revealed that the compound B6 had an identical antioxidant activity with α-Toc at the concentrations of 10, 25 and 50 μg/mL and higher efficiency at 100 μg/mL. It was also concluded that compounds B4, B5 and B7 demonstrated half antioxidant activity of with the BHT standard (Fig. 8).

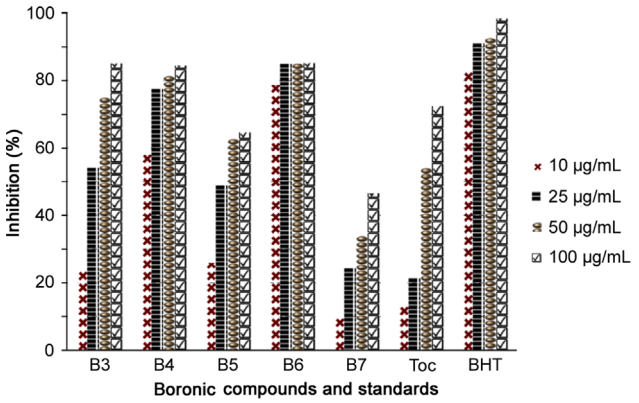

Fig. 5. Antioxidant activity of boronic compounds with β-carotene bleaching (BCB).

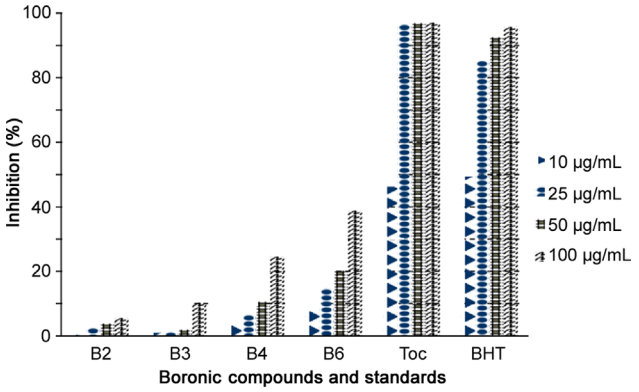

Fig. 6. Antioxidant activity of boronic compounds with 2,2-diphenyl picryl hydrazyl (DPPH).

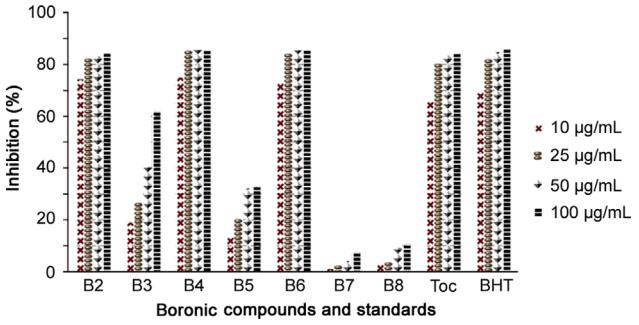

Fig. 7. Antioxidant activity of boronic compounds with 2,2′-azino-bis(3-ethylbenzothiazoline-6-sulphonic acid) (ABTS).

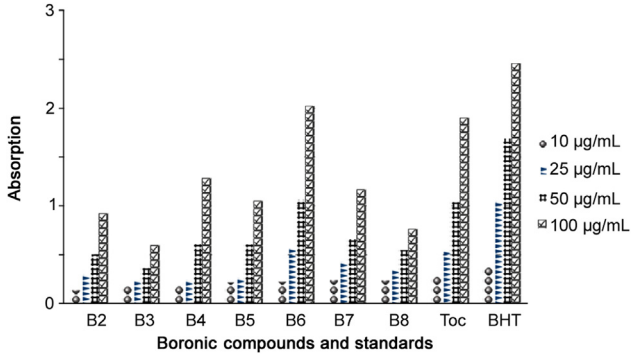

Fig. 8. Antioxidant activity of boronic compounds with CUPric reducing antioxidant capacity (CUPRAC).

4. Conclusions

In the present study, boronic compounds bearing imine were synthesized, identified and then employed for prostate cancer treatment. It was found that B5 and B7 demonstrated significant cytotoxic activity against the cancer cells whereas the healthy cells were protected by these compounds at higher percentages. The conclusion was drawn as these compounds can be promising candidates for drug design in cancer research. The antimicrobial features were studied by various microorganisms and B1 was found to be the most efficient compound with the different amount of growth inhibition zone against the four of these microorganisms. The antioxidant activities were investigated by the BCB, DPPH, ABTS and CUPRAC methods and the B6 displayed the highest antioxidant activity for all of these antioxidant assays. The best data was collected from the ABTS assay and compound B6 was reported better antioxidant agent than the two of the standards BHT and α-Toc.

Acknowledgments

Dicle University Science and Technology Research Center (DUBTAM) and Dicle University Scientific and Technological Research Council (DUBAP) with Grant Number: 14–EZF–14 are gratefully acknowledged for their analysis and financial supports.

References

[1] V.M. Dembitsky, R. Smoum, A.A. Al-Quntar, et al., Natural occurrence of boron-containing compounds in plants, algae and microorganisms, Plant Sci. 163 (2002) 931–942.
[2] G.S. Kelly, Boron: a review of its nutritional interactions and therapeutic uses, Altern. Med. Rev. 2 (1997) 48–56.
[3] S. Han, L.S. Chen, H.X. Jiang, et al., Boron deficiency decreases growth and photosynthesis, and increases starch and hexoses in leaves of citrus seedlings, J. Plant Physiol. 165 (2008) 1331–1341.
[4] D.L. Zhao, D.M. Oosterhuis, Cotton growth and physiological responses to boron deficiency, J. Plant Nutr. 26 (2003) 855–867.
[5] R. Kastori, M. Plesnicar, D. Panković, et al., Photosynthesis, chlorophyll fluorescence and soluble carbohydrates in sunflower leaves as affected by boron deficiency, J. Plant Nutr. 18 (1995) 1751–1763.
[6] V.M. Shorrocks, The occurrence and correction of boron deficiency, Plant Soil 193 (1997) 121–148.
[7] J.G. Penland, Dietary boron, brain function, and cognitive performance, Environ. Health Perspect. 102 (1994) 65–72.
[8] A.K. Azab, H.A. Ali, M. Srebnik, Chapter 5: Boron Neutron Capture Therapy, in: V.M.D. Hijazi Abu Ali, S. Morris (Eds.), Studies in Inorganic Chemistry, Elsevier, USA, 2006.
[9] J. Carlsson, L. Gedda, C. Grönvik, et al., Strategy for boron neutron capture therapy against tumor cells with over-expression of the epidermal growth factor-receptor, Int. J. Radiat. Oncol. Biol. Phys. 30 (1994) 105–115.
[10] L. Kankaanranta, T. Seppälä, H. Koivunoro, et al., Boron neutron capture therapy in the treatment of locally recurred head-and-neck cancer: final analysis of a phase I/II trial, Int. J. Radiat. Oncol. Biol. Phys. 82 (2012) e67–e75.
[11] W. Tjarks, The use of boron clusters in the rational design of boronated nucleosides for neutron capture therapy of cancer, J. Organomet. Chem. 614 (2000) 37–47.
[12] F. Rezaee, F. Ghanati, M. Behmanesh, Antioxidant activity and expression of catalase gene of (*Eustoma grandiflorum* L) in response to boron and aluminum, S. Afr. J. Bot. 84 (2013) 13–18.
[13] M. Landi, A. Pardossi, D. Remorini, et al., Antioxidant and photosynthetic response of a purple-leaved and a green-leaved cultivar of sweet basil (*Ocimum basilicum*) to boron excess, Environ. Exp. Bot. 85 (2013) 64–75.
[14] J.C. Melgar, L. Guidi, D. Remorini, et al., Antioxidant defences and oxidative damage in salt-treated olive plants under contrasting sunlight irradiance, Tree Physiol. 29 (2009) 1187–1198.
[15] L.M. Cervilla, B. Blasco, J.J. Ríos, et al., Oxidative stress and antioxidants in tomato (*Solanum lycopersicum*) plants subjected to boron toxicity, Ann. Bot. 100 (2007) 747–756.
[16] M. Tümer, H. Köksal, M.K. Sener, et al., Antimicrobial activity studies of the binuclear metal complexes derived from tridentate Schiff base ligands, Transit. Met. Chem. 24 (1999) 414–420.
[17] N. Raman, J.D. Raja, A. Sakthiveli, Synthesis, spectral characterization of Schiff base transition metal complexes: DNA cleavage and antimicrobial activity studies, J. Chem. Sci. 119 (2007) 303–310.
[18] R.K. Parashar, R.C. Sharma, A. Kumar, et al., Stability studies in relation to IR

data of some Schiff base complexes of transition metals and their biological and pharmacological studies, Inorg. Chim. Acta 151 (1988) 201–208.
[19] L. Shi, H.M. Ge, S.H. Tan, et al., Synthesis and antimicrobial activities of Schiff bases derived from 5-chloro-salicylaldehyde, Eur. J. Med. Chem. 42 (2007) 558–564.
[20] N. Raman, J.D. Raja, A. Sakthivel, Synthesis, spectral characterization of Schiff base transition metal complexes: DNA cleavage and antimicrobial activity studies, J. Chem. Sci. 119 (2007) 303–310.
[21] S. Kalaycı, S. Demirci, F. Sahin, Determination of antimicrobial properties of Picaridin and DEET against a broad range of microorganisms, World J. Microbiol. Biotechnol. 30 (2014) 407–411.
[22] N.C. Cook, S. Saman, Flavonoids-chemistry, metabolism, cardioprotective effects and dietary sources, J. Nutr. Biochem. 7 (1996) 66–76.
[23] B. Halliwell, Free radicals and antioxidants: a personal view, Nutr. Rev. 52 (1994) 253–265.
[24] C.T. Ho, Q. Chen, K.Q. Shi, et al., Antioxidative effect of polyphenol extract prepared from various Chinese teas, Prev. Med. 21 (1992) 520–525.
[25] M.J. Taylor, T. Richardson, Antioxidant activity of cysteine and protein sulfhydryls in a linoleate emulsion oxidized by hemoglobin, J. Food Sci. 45 (1980) 1223–1227.
[26] E. Yamazaki, M. Inagaki, O. Kurita, et al., Antioxidant activity of Japanese pepper (*Zanthoxylum piperitum* DC.) fruit, Food Chem. 100 (2007) 171–177.
[27] S. Arunachalam, N.P. Priya, C. Jayabalakrishnan, et al., Synthesis, spectral characterization, catalytic and antibacterial studies of new Ru(III) Schiff base complexes containing chloride/bromide and triphenylphosphine/arsine as co-ligands, Spectrochim. Acta Part A: Mol. Biomol. Spectrosc. 74 (2009) 591–596.
[28] M. Badertscher, P. Bühlmann, E. Pretsch, Structure Determination of Organic Compounds, 4th ed., Springer-Verlag, Berlin Heidelberg, 2008.
[29] B.T. Thaker, R.S. Barvalia, Ligating behaviour of Schiff base ligands derived from heterocyclic β-diketone and ethanol or propanol amine with oxovanadium (IV) metal ion, Spectrochim. Acta Part A: Mol. Biomol. Spectrosc. 74 (2009) 1016–1024.
[30] A. Oueslati, S. Kamouna, F. Hlel, et al., Real-time FTIR and electrical monitoring of the photopolymerization of a pentaerythritol triacrylate-based resin, Phys. Sci. 1 (2011) 1–6.
[31] J.A. Faniran, H.F. Shurvell, J.A. Faniran, et al., Infrared spectra of phenylboronic acid (normal and deuterated) and diphenyl phenylboronate, Can. J. Chem. 46 (1968) 2089–2095.
[32] A.N.M.A. Alaghaz, Synthesis, spectroscopic characterization, molecular modeling and potentiometric studies of Co(II), Ni(II), Cu(II) and Zn(II) complexes with 1,1-diaminobutane-Schiff base, J. Mol. Struct. 1072 (2014) 103–113.
[33] A.N.M.A. Alaghaz, Y.A. Ammar, H.A. Bayoumi, et al., Synthesis, spectral characterization, thermal analysis, molecular modeling and antimicrobial activity of new potentially N_2O_2 azo-dye Schiff base complexes, J. Mol. Struct. 1074 (2014) 359–375.
[34] M.I. Khan, A. Khan, I. Hussain, et al., Spectral, XRD, SEM and biological properties of new mononuclear Schiff base transition metal complexes, Inorg. Chem. Commun. 35 (2013) 104–109.
[35] M.S. Refat, M.Y. El-Sayed, A.M.A. Adam, Cu(II), Co(II) and Ni(II) complexes of new Schiff base ligand: synthesis, thermal and spectroscopic characterizations, J. Mol. Struct. 1038 (2013) 62–72.
[36] V. Barba, J. Vázquez, F. López, et al., Mono- and diboronates derived from tridentate ONO ligands and arylboronic acids, J. Organomet. Chem. 690 (2005) 2351–2357.
[37] A. Kilic, M. Aydemir, M. Durgun, et al., Fluorine/phenyl chelated boron complexes: synthesis, fluorescence properties and catalyst for transfer hydrogenation of aromatic ketones, J. Fluor. Chem. 162 (2014) 9–16.
[38] Y. Nagata, Y. Chujo, Main-chain-type N,N′-chelate organoboron aminoquinolate polymers: synthesis, luminescence, and energy transfer behavior, Macromolecules 41 (2008) 3488–3492.
[39] Y. Tokoro, A. Nagai, Y. Chujo, Synthesis of π-conjugated polymers containing organoboron benzo [h] quinolate in the main chain, Macromolecules 43 (2010) 6229–6233.
[40] D.M. Knapp, E.P. Gillis, M.D. Burke, A general solution for unstable boronic acids:slow-release cross-coupling from air-stable MIDA boronates, J. Am. Chem. Soc. 131 (2009) 6961–6963.
[41] A.K. Singh, S.K. Pandey, O.P. Pandey, et al., Synthesis and spectral characterization of Zn(II) microsphere series for antimicrobial application, J. Mol. Struct. 1074 (2014) 376–383.
[42] A. Kilic, C. Kayan, M. Aydemir, et al., Synthesis of new boron complexes: application to transfer hydrogenation of acetophenone derivatives, Appl. Organomet. Chem. 25 (2011) 390–394.
[43] M.A. Migahed, A.A. Farag, S.M. Elsaed, et al., Synthesis of a new family of Schiff base nonionic surfactants and evaluation of their corrosion inhibition effect on X-65 type tubing steel in deep oil wells formation water, Mater. Chem. Phys. 125 (2011) 125–135.
[44] K.M. Vyas, R.N. Jadeja, V.K. Gupta, et al., Synthesis, characterization and crystal structure of some bidentate heterocyclic Schiff base ligands of 4-toluoyl pyrazolones and its mononuclear Cu(II) complexes, J. Mol. Struct. 990 (2011) 110–120.
[45] K.R. Ansari, M.A. Quraishi, Bis-Schiff bases of isatin as new and environmentally benign corrosion inhibitor for mild steel, J. Ind. Eng. Chem. 20 (2014) 2819–2829.
[46] A. Kumar, M. Agarwal, A.K. Singh, et al., Palladium(II), platinum(II), ruthenium (II) and mercury(II) complexes of potentially tridentate Schiff base ligands of (E, N, O) type (E=S, Se, Te): Synthesis, crystal structures and applications in Heck and Suzuki coupling reactions, Inorg. Chim. Acta 362 (2009) 3208–3218.